Chinese Chemical Letters 37 (2026) 111957

Contents lists available at ScienceDirect

Chinese Chemical Letters

journal homepage: www.elsevier.com/locate/cclet

Recent advances in carbon dots imaging at the subcellular level: Synthesis strategies, properties, and organelle imaging

Xinjuan He[a], Zishuo Wang[a], Boyang Wang[b], Yongqiang Zhang[b], Xiaokai Xu[c,*], Huijuan Cai[a,*], Siyu Lu[b,*]

[a] Henan Institute of Advanced Technology, Zhengzhou University, Zhengzhou 450001, China
[b] College of Chemistry, Pingyuan Laboratory, Zhengzhou University, Zhengzhou 450001, China
[c] College of Chemistry and Phamaceutical Sciences, Qingdao Agricultural University, Qingdao 266109, China

ARTICLE INFO

Article history:
Received 31 March 2025
Revised 30 September 2025
Accepted 13 October 2025
Available online 14 October 2025

Keywords:
Carbon dots
Organelle targeting
Subcellular imaging
Photoluminescence
Mechanisms

ABSTRACT

Carbon dots (CDs), a class of emerging fluorescent nanomaterials, have garnered notable attention in the biomedical field owing to their outstanding photoluminescence properties, excellent biocompatibility, and ease of synthesis and functionalization. Recently, numerous CDs have been developed that allow precise subcellular localization through surface modifications or covalent conjugation with targeting ligands such as peptides, small molecules, Golgi-specific agents, and cell membrane-specific agents. This review begins with an overview of the synthesis strategies of CDs, highlighting their exceptional optical properties, stability, biocompatibility, and significance for subcellular imaging. The mechanisms by which CDs target specific organelles, including the nucleus, mitochondrion, lysosomes, Golgi apparatus, and cell membrane, are discussed. These mechanisms include specific targeting molecules, pH-sensitive targeting, charge-driven interactions, and hydrophobic and hydrophilic dynamics. Furthermore, we summarize their applications in subcellular imaging, such as the long-term dynamic monitoring of organelles, sensing, reactive oxygen species scavenging, and therapy. By presenting a comprehensive review of CDs in subcellular imaging, we aim to pave the way for further development of CDs in bioimaging and related biomedical applications.

© 2025 Published by Elsevier B.V. on behalf of Chinese Chemical Society and Institute of Materia Medica, Chinese Academy of Medical Sciences.

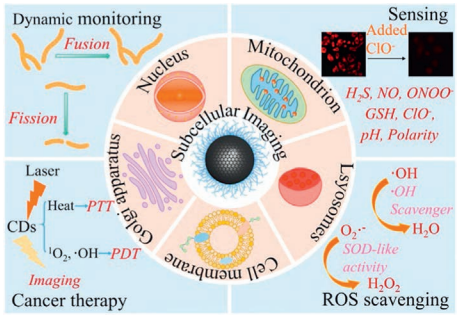
1. Introduction

Cells, the fundamental units of metabolism and function in living organisms, comprise complex and exquisite structures such as the cell membrane, cytoplasm, and nucleus [1]. These subcellular structural components are closely connected to highly organized life activities [2,3]. Therefore, precise imaging analysis at the subcellular level can provide valuable information regarding the changes in physiological activities and early diagnosis or timely treatment of relevant diseases. Among various imaging methods, fluorescence (FL) imaging is a simple and sensitive technique that can provide high resolution, numerous real-time signals and enable instant monitoring of microstructural and biomolecular dynamics in living cells [4]. Semiconductor quantum dots (QDs), upconversion nanoparticles, organic dyes, and fluorescent proteins have been widely employed as fluorescent nanoprobes for subcellular imaging [5,6]. However, because of their large size and low tissue penetration depth, they are not conducive for clinical treatment [7–9]. To this end, new nanomaterials with good biocompatibility, high stability, high quantum yield (QY) and small size must be designed as fluorescent probes for subcellular imaging; carbon dots (CDs) possess all of these advantages [10].

CDs are carbon-based zero-dimensional photoluminescence (PL) nanomaterials with a core-shell structure [11], consisting of the sp^2/sp^3 carbon framework and various surface functional groups, such as amino, epoxy, ether, carbonyl, hydroxyl, or organic molecules, or polymers [12]. CDs offer several advantages, including bright and visible FL, high QY, red/near-infrared (NIR) emission, excellent stability and biocompatibility [13,14]. These attributes make CDs suitable for high-resolution, long-term and full-color FL imaging applications. The ultra-small size of CDs allows them to function independently or integrate with other nanotherapeutics, thereby enhancing therapeutic effects. Unlike various conventional materials, CDs engage in human metabolic processes and are excreted renally post-administration [15]. Due to these exceptional properties, the biological applications of CDs have been extensively

* Corresponding authors.
E-mail addresses: xxk@qau.edu.cn (X. Xu), caihj10@zzu.edu.cn (H. Cai), sylu2013@zzu.edu.cn (S. Lu).

https://doi.org/10.1016/j.cclet.2025.111957
1001-8417/© 2025 Published by Elsevier B.V. on behalf of Chinese Chemical Society and Institute of Materia Medica, Chinese Academy of Medical Sciences.



Scheme 1. Subcellular level imaging of CDs and their further applications.

explored and applied in FL sensing, cell/tissue imaging, drug delivery, photodynamic therapy (PDT), and photothermal therapy (PTT) [16].

Generally, CDs can rapidly enter cells through endocytosis mediated by energy-dependent and temperature-dependent pathways (*e.g.*, macropinocytosis, clathrin, caveolae, or lipid raft), enabling efficient cellular imaging [17]. Certain CDs with unique structures accumulate in specific subcellular organelles, allowing subcellular imaging. For instance, Wang *et al.* [18] synthesized ultrabright green sulfur-doped CDs that enabled long-term stable endoplasmic reticulum (ER) imaging in living cells. Furthermore, the authors effectively discriminated between ER stress behaviors induced by different stimuli. The advancement of CDs in subcellular imaging enables specific visualization of the nucleus, mitochondrion, Golgi apparatus, lysosomes, and cell membrane, expanding their applications in dynamic monitoring, sensing, reactive oxygen species (ROS) scavenging, and cancer therapy (Scheme 1). Therefore, CDs have become a powerful tool for imaging organelles and insights into biological systems.

Many studies and reviews have been published on CDs for cellular imaging [16,19]. However, only a few reviews focused on subcellular imaging (including cell membrane and organelles). This review systematically explores the synthesis strategies of CDs and their inherent physicochemical advantages at the subcellular imaging, with a specific focus on subcellular imaging applications. First, two synthesis methods, one-step and multi-step methods for the preparation of organelle/membrane-specific CDs are discussed. The one-step process is a conventional route encompassing heteroatom doping and functional group/structure incorporation, while multi-step approach comprises covalent and non-covalent coupling strategies. Second, the PL properties of CDs (such as FL, up-conversion PL, room temperature phosphorescence (RTP) and photothermal properties) are presented. In addition, the typical advantages of CDs over other imaging agents are analyzed, including stability biocompatibility, and water solubility. This review comprehensively examines the applications of CDs in targeted subcellular imaging, with particular emphasis on elucidating the mechanisms underlying their organelle-specific targeting capabilities toward nucleus, mitochondrion, lysosomes, Golgi apparatus, and cell membrane. Their unique photophysical properties enable long-term dynamic monitoring of cellular processes including cell cycle progression, autophagy, and nucleolar stress responses, while simultaneously serving as versatile platforms for biosensing (toxicological assessment and ion detection), cancer theranostics (encompassing PDT, PTT, and drug delivery systems), and ROS scavenging for anti-inflammatory applications. By establishing systematic correlations between structural design principles and biological functionalities, this analysis offers foundational guidelines for developing next-generation CDs-based probes with enhanced targeting precision. Finally, challenges and future trends in the application of CDs for subcellular imaging are discussed. We anticipate that this comprehensive review will stimulate further research endeavors in CDs-based subcellular imaging and propel the development of organelle-specific nanoprobes for advanced biomedical applications.

2. Synthesis methods

Various methods can synthesize different types of CDs. Their microstructures can be subdivided into four categories: Graphene quantum dots (GQDs), carbon quantum dots (CQDs), carbon nanodots (CNDs), and carbonized polymer dots (CPDs). The carbon core of the GQDs has a two-dimensional layered graphene core with several chemical groups at the edges [20]. CQDs have a graphite-like crystal lattice, a spherical core, and surface chemical groups [20,21]. CNDs exhibit spherical morphologies with surface-functionalized chemical groups, while their amorphous cores distinguish them structurally from CQDs [21,22]. CPDs exhibit a lower degree of carbonization and have a carbon/polymer hybrid skeleton, numerous functional groups/polymer chains in both carbon core and shell, a highly dehydrated crosslinked polymer framework, and a slightly graphite core [15,22,23]. In addition to structural variations, these carbon-based nanomaterials exhibit distinct PL origins: CQDs demonstrate quantum confinement-driven emission [20], whereas CNDs derive PL from surface defect states or molecular fluorophores [21]. GQDs display edge state and sp^2-conjugation dependent luminescence [21], while CPDs rely on molecular state luminescence and cross-linked enhanced emission effect [24]. All four share carbon-centric compositions, tunable PL properties, and broad applicability in bioimaging, energy conversion, and sensing technologies. CDs can be developed using various carbon sources, ranging from bulk carbon materials to biomass and small molecules [25–27]. In general, the diversity of carbon precursors and synthesis strategies determines the structural and functional variations of synthesized CDs, enabling their versatile applications [28]. In this review, CDs synthesis strategies applied in subcellular imaging are summarized and classified into one-step and multi-step methods. The specific details are summarized in Supporting information.

3. Properties

The PL properties of CDs are one among their advantages. Most CDs exhibit FL characteristics derived from their singlet state, which are more commonly observed in subcellular imaging. Compared with QDs and organic fluorescent dyes, CDs can maintain high PL behavior even under complex external conditions (such as acidity and alkalinity, high temperature, and high salinity) or continuous light stimulation, because most CDs have a stable sp^2 carbon skeleton structure. Excellent PL properties and photostability are the basis for using CDs in subcellular imaging. The composition and structure of CDs determine their unique optical properties, including FL, up-conversion PL, RTP and photothermal properties.

Detailed data on the optical properties and biocompatibility of CDs engineered to image subcellular structures are provided in Supporting information.

4. Imaging applications at the subcellular level

Various cellular components, including the nucleus, cell membrane, and organelles (such as mitochondrion, lysosomes, and the Golgi apparatus), are key units responsible for sustaining life through specific biochemical processes. Accurate imaging analysis of these cellular components enables researchers to precisely characterize molecular, biochemical, and physiological processes underlying disease mechanisms, embryonic development, tissue dif-

ferentiation, aging, and pathogen responses [29,30]. This approach significantly contributes to understanding disease progression associated with these processes, including cancer, Alzheimer's disease, Parkinson's disease, diabetes, and cardiovascular disorders [31]. Subcellular structures exhibit distinct membrane characteristics and internal biochemical properties. Given these distinct features, researchers have developed CDs with target-specific modifications by tailoring their size, functional groups, and surface charge during synthesis, achieving precise localization at subcellular membranes or controlled internalization [6]. The comprehensive details of CDs enabling lysosomes, Golgi apparatus, and cell membrane targeted imaging and their applications are summarized in Supporting information.

4.1. Cell nucleus

The nucleus, mainly composed of chromatin (containing DNA) and nucleolus (containing RNA), is the largest and most prominent subcellular structure in eukaryotic cells. As the regulatory center of genetic control and cellular metabolism, the nucleus coordinates RNA synthesis, processing, and ribosome assembly, while also governing cellular metabolism, growth, and differentiation [32]. Some biological processes, including apoptosis, neurodegenerative and neuropsychiatric diseases, are related to the morphological and structural alterations of the nucleus [33]. Therefore, imaging of the nucleus is important for the visualization and direction of disease treatment.

CDs can stain the entire nucleus or selectively bind to DNA and nucleoli (RNA-rich regions). Xu *et al.* [34] synthesized red luminescent CDs using nitrogen-containing precursors. where elevated nitrogen content endowed the CDs with nuclear-targeting capability [35]. Additionally, it was also possible to achieve nucleolus imaging in live organ. *In vivo* toxicity of Ag^{+} could be assessed by observing morphological changes in the nucleolus and the FL intensity in cells (Fig. 1A). Jiang *et al.* [36] synthesized NIR fluorescent N-CDs-F, which bind to several RNA-containing ribosomes and ribonucleoproteins produced in the nucleus and cytoplasm of rapidly proliferating cancer cells, thereby efficiently staining of both nucleolar and cytoplasm region (Fig. 1B). Although CDs also stained the cytoplasm due to RNA, the staining pattern was distinct from that of the nucleolus. Cationic CDs contain abundant positively charged surface groups that electrostatically interact with negatively charged nuclear membranes, while their ultra-small size enables penetration into nucleoli [37]. For instance, Hua *et al.* [38] synthesized metal-free red fluorescent CDs by adding Ni^{2+} as a catalyst during the hydrothermal treatment of *p*-phenylenediamine, achieving nucleic acid targeting *via* electrostatic interactions.

The nucleolus is a central hub that coordinates cellular stress responses and various functions during cancer development and treatment. Characterization of nucleolar stress is crucial for the diagnosis and treatment of nucleolus-associated pathologies [39]. He *et al.* [40] synthesized CDs with integrated fluorescent blinking domains and RNA-binding motifs to imitate RNA-binding proteins in their structures. Furthermore, they confirmed that 1,2,3,5-tetrahydro-5-oxo-imidazo[1,2-α]pyridine-7-carboxylic acid fluorophores or its derivatives on the surface of CDs were RNA-binding motif groups. Using enhanced super-resolution imaging of nucleolar ultrastructure, researchers demonstrated that CDs can recognize and differentiate nucleolar responses to various stressors. The red fluorescent M-CDs prepared by Jiang *et al.* [41] retained part of the levofloxacin structure on their surface and inserted into the hairpin loop of RNA through hydrophobic and electrostatic interactions. M-CDs enabled rapid, wash-free, and highly-efficient RNA real-time imaging in the nucleolus of living cells (Fig. 1C). In addition, RNA aggregated with proteins to form stress granules (SGs) under stress conditions. Therefore, utilizing M-CDs enabled real-time imaging of the dynamic process under oxidative stress and revealed the structure of SGs.

In addition, CDs can directly monitor the cell-cycle by targeting the nucleoli and chromosomes and display the entire cell division process in real-time. For instance, the F and N co-doped CDs prepared by Li *et al.* [42] bound to nucleic acids through electrostatic interactions. Additionally, the fluorine component facilitated hydrogen bond formation, enabling their application as cell-cycle imaging probes. If nuclear staining enables the distinction between DNA and RNA, real-time monitoring of both nucleic acids would significantly facilitate cellular behavior analysis. Han *et al.* [43] have reported cationic CQDs containing several carboxyl groups. The structurally rigid double-stranded DNA (dsDNA) confined CQDs within its grooves, enhancing green FL from isolated particles. In contrast, flexible single-stranded RNA (ssRNA) induced CQD aggregation, leading to red-shifted FL emission (Fig. 1D). This enabled real-time monitoring of DNA and RNA localization and dynamics within cells.

Several reports have demonstrated the anticancer potential of CDs, achieved either through intrinsic CDs activity or by synergistically linking CDs to antitumor drugs for enhanced *in vivo* efficacy [44,45]. The nucleus manages the genetic information and protein transcription of the cell, making it an ideal target for the treatment of malignancies [46]. DOX is broadly used as an anthracycline antibiotic with extensive antitumor effects. It disrupts DNA replication in the nucleus and induces immunogenic cell death in tumor cells [47,48]. Li *et al.* [49] doped N/S elements to increase the conjugated structure of CDs, producing orange fluorescent CDs modified with NLS and DOX. Upon targeting the nuclei of liver cancer cells, the CDs released DOX within the acidic tumor microenvironment, exerting anticancer effects (Fig. 1E). Chen *et al.* [50] synthesized cationic CDs, where both intercalative binding and electrostatic interactions with DNA enabled nuclear imaging. Moreover, The CDs inhibited focal adhesion kinase overexpression in cancer cells and possess anticancer potential.

Altogether, according to previous studies (Table S1 in Supporting information), three methods of targeting CDs to the nucleus have been summarized: (1) Modifying CDs with NLS, (2) designing cationic CDs to bind with negatively charged nucleic acids *via* electrostatic interactions, and (3) attaching them to nucleic acids *via* amino groups. The detailed mechanisms of CDs targeting the cell nucleus remain unclear. Furthermore, studies on CDs capable of distinguishing between DNA and RNA imaging simultaneously remain relatively scarce and additional applications need to be expanded urgently.

4.2. Mitochondrion

Possessing their own genome and the ability to generate adenosine triphosphate *via* respiration, mitochondria serve as metabolic hubs where carbohydrates, lipids, and amino acids undergo oxidation to release energy [51]. Mitochondria are also involved in various life processes that regulate cellular metabolism, including the tricarboxylic acid cycle, oxidative phosphorylation, calcium ion storage, membrane potential regulation, iron-sulfur complex synthesis, programmed cell death, and modulation of cell proliferation [52]. Furthermore, they overproduce ROS, leading to oxidative cellular damage [53]. Mitochondrial damage and dysfunction have been implicated in aging and pathologies, such as cancer and Alzheimer's disease [54]. Consequently, sustained monitoring of mitochondrial function and dynamics is critical for modulating cell fate decisions and developing therapies for mitochondrial disorders. Zhu *et al.* [55] synthesized multicolor fluorescent CDs by adjusting the ratios of β-cyclodextrin and oPD to provide

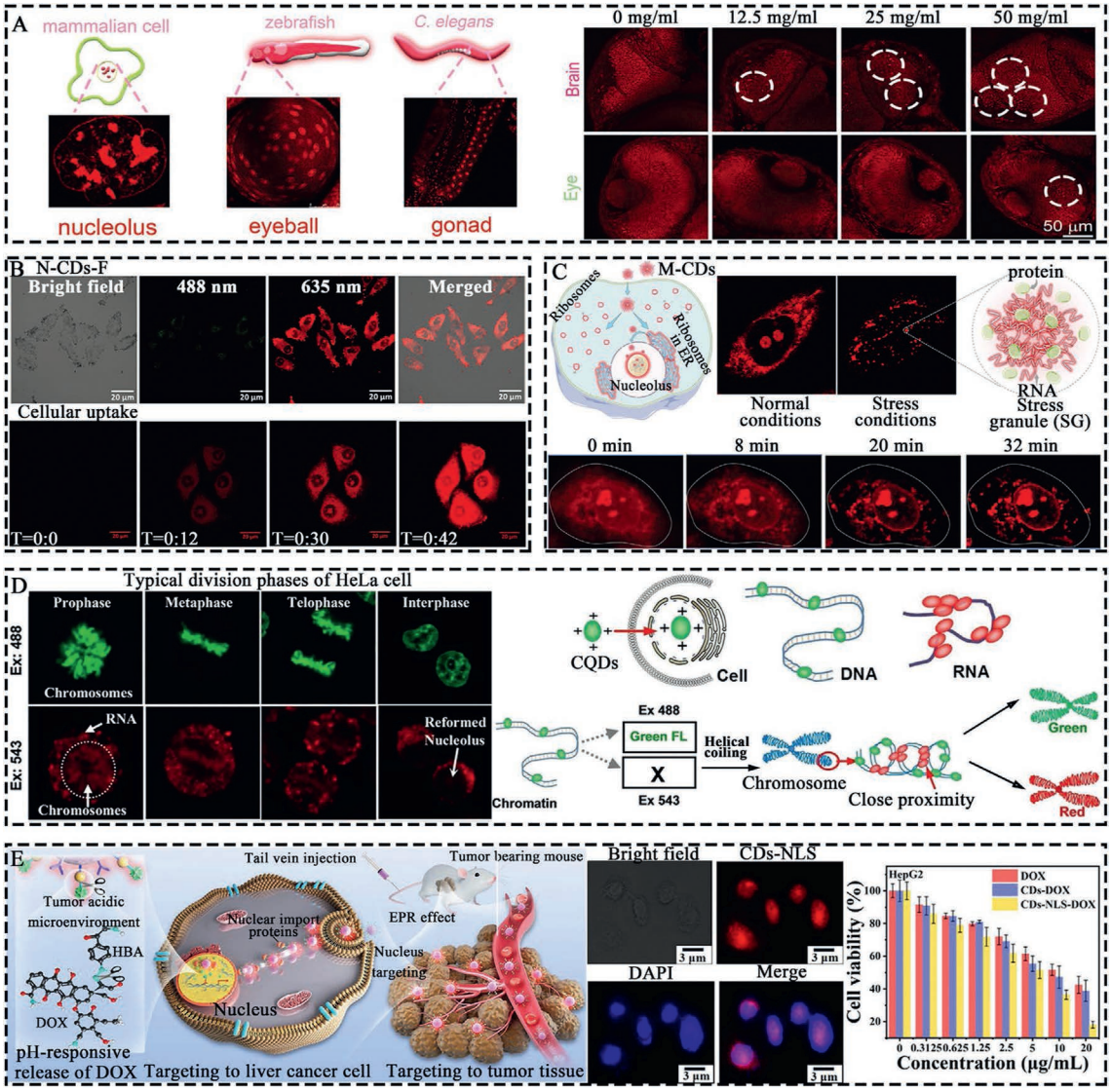


Fig. 1. CDs for nuclear imaging. (A) CDs utilized for both *in vitro* and *in vivo* FL imaging, as well as for evaluating Ag^{+}-induced toxicity. Reproduced with permission [34]. Copyright 2023, Wiley Publishing Group. (B) FL imaging of cells co-incubated with N-CDs-F and their internalization into cells. Reproduced with permission [36]. Copyright 2020, Wiley Publishing Group. (C) A schematic of M-CDs internalizing into RNA for imaging and monitoring the cellular oxidative stress process. Reproduced with permission [41]. Copyright 2023, Wiley Publishing Group. (D) CQDs-enabled imaging of nuclear dynamics throughout the cell division cycle, coupled with mechanistic demonstration of their targeting capabilities for DNA and RNA. Reproduced with permission [43]. Copyright 2019, Wiley Publishing Group. (E) Targeted therapeutic process of CDs-NLS-DOX in liver cancer, cell nuclear imaging and *in vitro* antitumor effect. Reproduced with permission [49]. Copyright 2024, Elsevier Publishers.

amino/hydroxyl functional groups, which enabling purple, blue, and green fluorescent imaging upon mitochondrial targeting.

Liu *et al.* [56] reported red-fluorescent CDs exhibiting superoxide dismutase (SOD) nanozyme activity. The nitrogen-doped surface and multifunctional groups enabled these CDs to traverse oxidatively damaged cell membranes, target mitochondria, and subsequently localize to lysosomes *via* endocytosis, achieving dual subcellular imaging and antioxidant cytoprotection (Fig. 2A). The catalytic mechanism of SOD involved hydroxyl, carboxyl, and amino groups on the CDs surface. These functional groups bind superoxide radicals through hydrogen bonding, facilitating electron transfer and promoting the dismutation of superoxide radicals into molecular oxygen and hydrogen peroxide. When intervertebral discs are injured or irritated, the hypoxic microenvironment maintained by annulus fibrosus and cartilage endplates surrounding nucleus pulposus cells becomes disrupted. This triggers abnormal ROS accumulation, ultimately driving the pathogenesis of intervertebral disc degeneration (IVDD), a prevalent degenerative musculoskeletal disorder [57,58]. In recent years, Prussian blue (PB) nanoparticles have demonstrated the ability to mimic the antioxidant activities of SOD and catalase (CAT), efficiently scavenging harmful ROS *via* catalytic conversion into non-toxic products [59] Simultaneously, Fe^{2+} on the surface of PB directly react with hydroxyl radical ($^{\bullet}OH$), scavenging these free radicals and thereby inhibiting oxidative reactions. Given this, Shi *et al.* [60] reported that PB-loaded CDs with modified TPP ligands (CD-PB-TPP) could target the mitochondrion for imaging and significantly reduce ROS levels, thereby rescuing impaired mitochondria function and protecting nucleus pulposus cells from aging and inflammation (Fig. 2B). Studies have shown that mitochondrial dysfunction and dysregulated dynamics can trigger iron metabolism disorders. Specifically, iron overload generates excessive ROS *via* Fenton reactions, which disrupt mitochondrial membrane integrity and exacerbate functional impairment [61]. Selenium-doped CDs (SeCDs) with ROS-scavenging ability prepared by Zhang *et al.* [62] were efficiently enriched in mitochondrion. They restored mitochondrial

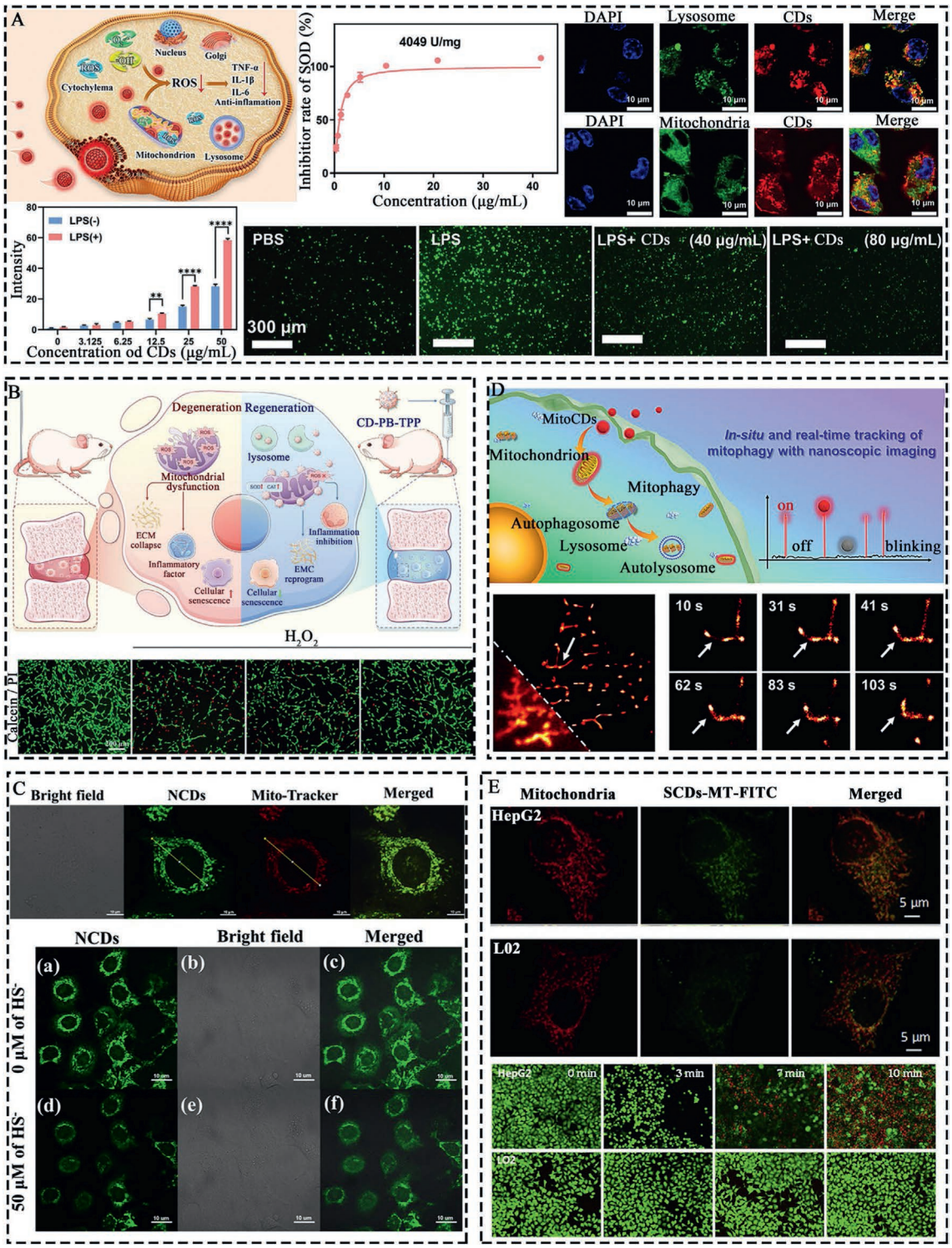


Fig. 2. CDs for mitochondrial imaging. (A) Schematics of ROS scavenging by CDs and mitochondrial imaging. Reproduced with permission [56]. Copyright 2023, Wiley Publishing Group. (B) CD-PB-TPP alleviates IVDD by targeting mitochondrion to clear ROS. Reproduced with permission [60]. Copyright 2024, Wiley Publishing Group. (C) Mitochondrial imaging and HS^- detection of NCDs. Reproduced with permission [65]. Copyright 2022, Elsevier Publishers. (D) Synthesis route of MitoCD and schematic mitochondrial autophagy tracking by nanoimaging. Reproduced with permission [71]. Copyright 2019, American Chemical Society. (E) Specific targeting of SCDs-MT to the mitochondrion of cancer cells and PTT against cancer. Reproduced with permission [74]. Copyright 2020, Elsevier Publishers.

function through multi-hierarchy iron chelation, mitochondrial iron chelation, ROS scavenging, and upregulation of glutathione peroxidase 4, effectively inhibiting ferroptosis and alleviating inflammatory responses. Moreover, SeCDs rescued the osteogenic differentiation capacity of stem cells, reversing the impairment induced by ferroptosis.

In addition to being modified with TPP molecules for mitochondrial targeting, cationic CDs are driven by the high mitochondrial membrane potential (MMP: −180 mV to −200 mV) to accumulate in the inner mitochondrial membrane [63]. Hydrogen sulfide (H_2S) is considered to be the third endogenous gaseous signaling molecule following carbon monoxide (CO) and nitric oxide (NO),

which modulate cellular processes and regulate physiological functions in humans [64]. Cai *et al.* [65] prepared positively charged NCDs that accumulate in mitochondria of living cells through electrostatic interactions. Moreover, HS^- is adsorbed on NCDs surface *via* non-covalent interactions, enabling detection of exogenous HS^- in the mitochondria (Fig. 2C). Similarly, ClO^- plays a vital role in physiological activities, but its overaccumulation is linked to diseases such as oxidative stress-related disorders, mental illnesses, and rheumatoid arthritis [66]. Cheng *et al.* [67] synthesized CDs incorporating lipophilic cations that enable sensitive ClO^- detection with specific mitochondrial targeting capabilities.

Inspired by conventional lipophilic cationic rhodamine probes relying on electrostatic interactions, Geng *et al.* [68] devised CDs exhibiting green-to-red emission with the lipophilic cation of rhodamine-derived as the luminescent centers. These CDs have been successfully applied for mitochondrion-targeted imaging of HeLa cells with tracking capability spanning six cell generations. Morphological changes in the mitochondria including fusion and fission, are rapid and long-term dynamic processes that play vital roles for maintaining cellular homeostasis. Abnormalities in mitochondrial dynamics are closely associated with neurodegenerative diseases, inflammation, metabolic disorders, and cancer [69,70]. Hence, Ye *et al.* [71] developed MitoCD, a thiol-based reaction-free mechanism for targeting the mitochondria without depleting the thiol groups of mitochondrial proteins (Fig. 2D). This probe enabled real-time observation of mitochondrial fission, fusion dynamics, and mitophagy monitoring in living cells. This study provided insights into mitochondrial metabolism while demonstrating the feasibility of using MitoCD for long-term nanoscale imaging of live cells. Xin *et al.* [72] designed orange fluorescent CDs (O-CDs) with hydroxyl and ammonium groups enriched, enabling mitochondria-specific accumulation *via* electrostatic targeting. In this case, the FL attenuation observed upon MMP reduction suggested hydrogen bonding interactions between hydroxyl/amino groups on mitochondrial proteins and thiol-containing molecules. Beyond monitoring mitochondrial fission and fusion dynamics in HeLa cells, O-CDs could also visualize the dynamic interactions between mitochondria and lipid droplets (LDs) during apoptosis and mitophagy, enabling long-term tracking of mitochondrial dynamics.

Apart from performing central bioenergetic functions, mitochondria supply metabolic precursors for tumor anabolism, redox processes, calcium homeostasis, transcriptional regulation, and programmed cell death [73]. This multifunctionality establishes mitochondria as promising targets for CDs-based anticancer therapies. Shen *et al.* [74] prepared smart CDs (SCDs) capable of acidic condition-induced self-assembly into aggregated states. The CDs (designated SCDs-MT) were surface-functionalized with mitochondria-targeting and cancer-cell-targeting peptides. SCDs-MT accumulated specifically in the mitochondrion of HepG2 cells and achieved precise cancer cell ablation through PTT (Fig. 2E). Additionally, Xiang *et al.* [75] reported NIR light-triggered upconversion of CDs conjugated to porphyrin-like porous MOFs surfaces, which were further functionalized with the mitochondria-targeting ligand TPP. This design enabled precise mitochondrial imaging and enhanced mitochondria-targeted PDT.

In summary, we conclude that CDs are competent for targeted mitochondrial imaging to detect variations in ion concentrations within the mitochondrion, monitor mitochondrial dynamics, scavenge ROS and eliminate cancer cells (Table S2 in Supporting information). According to previous research, we categorized three strategies for imaging mitochondrion using CDs: (1) TPP conjugation, (2) electrostatic targeting *via* cationic CDs, and (3) mitochondria-targeting peptide functionalization. Given mitochondria's central role in cellular physiology, real-time tracking of their multifunctional activities remains essential.

5. Conclusions and perspectives

CDs are emerging as promising alternatives to conventional subcellular markers (*e.g.*, nucleus, mitochondria, lysosomes, Golgi apparatus, and cell membrane) owing to their high water solubility, excellent biocompatibility, tunable FL properties, facile synthesis, and versatile functionalization. Nevertheless, significant challenges persist in organelle-specific imaging applications, as outlined below.

(1) Most currently developed CDs have been primarily engineered for the visible spectral range. However, imaging within this visible region faces to serious damage and has low penetration depth in biological tissues. Therefore, it is necessary to develop CDs with high QY, NIR absorption and luminescence properties.
(2) While subcellular targeting molecules (*e.g.*, TPP, ML, NLS) have been well-characterized, systematic principles for designing precursor materials to confer CDs with organelle-specific targeting capabilities remain undefined, and the mechanisms governing their targeting specificity are yet to be fully elucidated.
(3) The development of multifunctional CDs capable of targeted imaging and other physiological functions (*e.g.* regulation of cell physiological behaviors such as proliferation, differentiation, apoptosis, and monitoring of intracellular material recycling) remains a significant challenge. Furthermore, research on CDs with therapeutic effects remains relatively scarce.
(4) Researchers have mainly focused on the nucleus, mitochondrion, and lysosomes at the subcellular level, whereas the Golgi apparatus, LDs, ER, ribosomal centrosomes, cell membrane, peroxisomes, and phagosomes remain significantly understudied.

We believe that CDs with excellent optical performance will be developed to emerge as versatile platforms for subcellular-targeted imaging, physiological monitoring, and organelle-specific therapeutic applications in the future.

Declaration of competing interest

The authors declare that they have no known competing financial interests or personal relationships that could have appeared to influence the work reported in this paper.

CRediT authorship contribution statement

Xinjuan He: Writing – original draft, Investigation, Formal analysis. **Zishuo Wang:** Writing – original draft, Software, Methodology. **Boyang Wang:** Software, Methodology. **Yongqiang Zhang:** Methodology, Investigation, Formal analysis. **Xiaokai Xu:** Writing – review & editing. **Huijuan Cai:** Formal analysis, Data curation. **Siyu Lu:** Visualization, Project administration, Funding acquisition.

Acknowledgment

This work acknowledges the financial support received from the National Natural Science Foundation of China (No. U24A2079).

Supplementary materials

Supplementary material associated with this article can be found, in the online version, at doi:10.1016/j.cclet.2025.111957.

References

[1] D.E. Gottschling, T. Nystrom, Cell 169 (2017) 24–34.
[2] N. Chou, H. Shin, K. Kim, et al., Adv. Sci. 9 (2022) 2103564.
[3] H. Fang, Y. Chen, Z. Jiang, W. He, Z. Guo, Acc. Chem. Res. 56 (2023) 258–269.
[4] E.A. Specht, E. Braselmann, A.E. Palmer, Annu. Rev. Physiol. 79 (2017) 93–117.
[5] H. Ali, S. Ghosh, N. Jana, WIREs Nanomed. Nanobiotechnol. 12 (2020) e1617.

[6] B. Unnikrishnan, R.S. Wu, S.C. Wei, C.C. Huang, H.T. Chang, ACS Omega 5 (2020) 11248–11261.
[7] V.G. Reshma, P.V. Mohanan, J. Lumin. 205 (2019) 287–298.
[8] B. Chen, F. Wang, Trends Chem. 2 (2020) 427–439.
[9] F. An, N. Chen, W. Conlon, et al., Int. J. Biol. Macromol. 153 (2020) 100–106.
[10] C. Shen, Q. Lou, K. Liu, L. Dong, C. Shan, Nano Today 35 (2020) 100954.
[11] B. Wang, Z. Wei, L. Sui, et al., Light Sci. Appl. 11 (2022) 172.
[12] Z. Peng, X. Han, S. Li, et al., Coord. Chem. Rev. 343 (2017) 256–277.
[13] Y. Zhang, S. Lu, Chem 10 (2024) 134–171.
[14] L. Shi, L. Ding, Y. Zhang, S. Lu, Nano Today 55 (2024) 102200.
[15] Y. Jiang, T. Zhao, W. Xu, Z. Peng, Carbon 219 (2024) 118838.
[16] B. Wang, H. Cai, G.I.N. Waterhouse, et al., Small Sci. 2 (2022) 2200012.
[17] Y. Song, C. Zhu, J. Song, et al., ACS Appl. Mater. Interfaces 9 (2017) 7399–7405.
[18] Z. Wang, K.F. Xu, G. Wang, et al., Chem. Eng. J. 457 (2023) 140997.
[19] C. Shen, H. Liu, Q. Lou, et al., Theranostics 12 (2022) 2860–2893.
[20] J. Liu, R. Li, B. Yang, ACS Cent. Sci. 6 (2020) 2179–2195.
[21] S. Li, L. Li, H. Tu, et al., Mater. Today 51 (2021) 188–207.
[22] C. Xia, S. Zhu, T. Feng, M. Yang, B. Yang, Adv. Sci. 6 (2019) 1901316.
[23] Y. Ru, G.I.N. Waterhouse, S. Lu, Aggregate 3 (2022) e296.
[24] J. Li, X. Gong, Small 18 (2022) 2205099.
[25] N. Wang, A. Zheng, X. Liu, et al., ACS Appl. Mater. Interfaces 10 (2018) 7901–7909.
[26] T.C. Wareing, P. Gentile, A.N. Phan, ACS Nano 15 (2021) 15471–15501.
[27] R. González-González, L. González, M. Madou, et al., Nanomaterials 12 (2022) 298.
[28] E. Liu, J. Wu, T. Liang, et al., Chin. J. Chem. 41 (2023) 1994–2001.
[29] C.P. Satori, M.M. Henderson, E.A. Krautkramer, et al., Chem. Rev. 113 (2013) 2733–2811.
[30] J. Huang, P. Meng, C. Wang, Y. Zhang, L. Zhou, Theranostics 12 (2022) 2445–2464.
[31] R. Yao, C. Ren, Z. Xia, Y. Yao, Autophagy 17 (2021) 385–401.
[32] R. Boon, G.G. Silveira, R. Mostoslavsky, Nat. Metab. 2 (2020) 1190–1203.
[33] A. Parra-Damas, C.A. Saura, Biol. Psychiatry 86 (2019) 87–96.
[34] K. Xu, H. Jia, Z. Wang, et al., Small 19 (2023) 2205890.
[35] L. Wang, M. Li, Y. Li, et al., Carbon 180 (2021) 48–55.
[36] L. Jiang, H. Ding, M. Xu, et al., Small 16 (2020) 2000680.
[37] L. Yue, Y. Wei, J. Fan, et al., New Carbon Mater. 36 (2021) 373–389.
[38] X. Hua, Y. Bao, J. Zeng, F. Wu, ACS Appl. Mater. Interfaces 11 (2019) 32647–32658.
[39] P. Tan, T. Hong, X. Cai, et al., Nucleic Acids Res. 50 (2022) e69.
[40] H. He, X. Chen, Z. Feng, et al., Nano Lett. 21 (2021) 5689–5696.
[41] L. Jiang, H. Cai, W. Zhou, et al., Adv. Mater. 35 (2023) 2210776.
[42] H. Li, H. Wang, J. Guo, et al., Sens. Actuator. B: Chem. 311 (2020) 127891.
[43] G. Han, J. Zhao, R. Zhang, et al., Angew. Chem. Int. Ed. 58 (2019) 7087–7091.
[44] T. Feng, X. Ai, G. An, P. Yang, Y. Zhao, ACS Nano 10 (2016) 4410–4420.
[45] S. Li, W. Su, H. Wu, et al., Nat. Biomed. Eng. 4 (2020) 704–716.
[46] L. Pan, J. Liu, J. Shi, Chem. Soc. Rev. 47 (2018) 6930–6946.
[47] X. Liu, Z. Zhao, X. Xu, et al., Adv. Funct. Mater. 35 (2024) 2416406.
[48] C.F. Thorn, C. Oshiro, S. Marsh, et al., Pharmacogenet. Genomics 21 (2011) 440–446.
[49] Q. Li, J. Fan, H. Mu, et al., Chin. Chem. Lett. 35 (2024) 108947.
[50] J. Chen, F. Li, J. Gu, et al., J. Colloid Interface Sci. 637 (2023) 193–206.
[51] J. Rahman, S. Rahman, Lancet 391 (2018) 2560–2574.
[52] R.P. Chakrabarty, N.S. Chandel, Cell Stem Cell 28 (2021) 394–408.
[53] D.C. Wallace, Nat. Genet. 50 (2018) 1642–1649.
[54] K.F. Macleod, Annu. Rev. Cancer Biol. 4 (2020) 41–60.
[55] P. Zhu, W. Li, Y. Zhang, et al., Chin. Chem. Lett. 34 (2023) 108239.
[56] C. Liu, W. Fan, W.X. Cheng, et al., Adv. Funct. Mater. 33 (2023) 2213856.
[57] S. He, N. Sharpless, Cell 169 (2017) 1000–1011.
[58] W. Yang, K. Li, Q. Pan, et al., ACS Nano 18 (2024) 3053–3072.
[59] C. Rizzo, F. Arcudi, L. Đorđević, et al., ACS Nano 12 (2018) 1296–1305.
[60] Y. Shi, W. Bu, D. Chu, et al., Adv. Healthcare Mater. 13 (2024) 2303206.
[61] J. Yin, X. Zheng, Y. Zhao, et al., Angew. Chem. Int. Ed. 63 (2024) e202402537.
[62] K. Zhang, X. Mao, H. Zhao, et al., Chem. Eng. J. 499 (2024) 156544.
[63] S.S. Liew, X. Qin, J. Zhou, et al., Angew. Chem. Int. Ed. 60 (2021) 2232–2256.
[64] H. Kimura, Antioxid. Redox Signal. 20 (2014) 783–793.
[65] H. Cai, A. Liu, M. Zhang, et al., Sens. Actuator. B: Chem. 367 (2022) 132048.
[66] N.A. Burmistrova, R.J. Meier, S. Schreml, A. Duerkop, Sens. Actuator. B: Chem. 193 (2014) 799–805.
[67] B. Cheng, L. Cao, C. Li, et al., Chin. Chem. Lett. 35 (2024) 108969.
[68] X. Geng, Y. Sun, Z. Li, et al., Small 15 (2019) 1901517.
[69] D.C. Chan, Annu. Rev. Pathol. Mech. Dis. 15 (2020) 235–259.
[70] L. Tábara, M. Segawa, J. Prudent, Nat. Rev. Mol. Cell Biol. 26 (2024) 123–146.
[71] Z. Ye, L. Wei, X. Geng, et al., ACS Nano 13 (2019) 11593–11602.
[72] N. Xin, D. Gao, B. Su, et al., ACS Sens. 8 (2023) 1161–1172.
[73] P.E. Porporato, N. Filigheddu, J.M.B. Pedro, G. Kroemer, L. Galluzzi, Cell Res. 28 (2018) 265–280.
[74] Y. Shen, X. Zhang, L. Liang, et al., Carbon 156 (2020) 558–567.
[75] Q. Xiang, W. Li, Y. Tan, et al., Chem. Eng. J. 444 (2022) 136706.